



**POLITECNICO**  
MILANO 1863

SCUOLA DI INGEGNERIA INDUSTRIALE  
E DELL'INFORMAZIONE

EXECUTIVE SUMMARY OF THE THESIS

## Sizing, Optimisation and Thermal Evaluation of an Axial Flux Permanent Magnet Motor in Comparison with a Radial Flux Motor

LAUREA MAGISTRALE IN AUTOMATION AND CONTROL ENGINEERING  
INGEGNERIA DELL'AUTOMAZIONE

**Author:** FRANCESCA NAVA

**Advisor:** PROF. FRANCESCO CASTELLI DEZZA

**Academic year:** 2022-2023

---

### Introduction

This thesis presents a research project focused on the development of more efficient electric motors for automotive use, supporting the transition to electric vehicles. The study includes the creation of innovative axial and radial flux motors, parameter optimisation, thermal evaluation, and performance comparisons, offering valuable insights for future electric vehicle development.

Transportation role in emissions and air pollution is critical. In 2021, the EU average was 116.3 grams of CO<sub>2</sub> per kilometre, with Italy at 124.6 grams. The National Recovery and Resilience Plan (PNRR), part of the European Next Generation EU project, allocates 750 billion euros to drive growth and sustainable mobility. It includes expanding cycle lanes, tram networks, and introducing zero-emission buses. High-power electric motors for the automotive industry are a key focus in achieving a sustainable transportation future.

In this thesis, a high-performance axial flux motor model will be built from scratch through optimisation using MATLAB and compared with a radial flux motor created in Ansys MotorCAD by modifying the well-known model of the Nissan Leaf. Notably, this project involved acquiring expertise in the use of four new software tools: MATLAB for model generation, ANSYS Maxwell, MotorXp and Ansys MotorCAD for result validation, and ANSYS Fluent for thermal result validation.

### 1. Comparison between Axial and Radial Flux Machines

Axial and radial flux electric machines present distinct design approaches for electric motors, particularly in automotive applications. Axial flux machines, characterised by a compact, pancake-like design and parallel magnetic flux to the rotational axis, offer higher power density and efficiency, but may necessitate more complex cooling and winding arrangements. In contrast, radial flux machines have a reliable but bulkier design, with limitations in power density. Axial flux motors, featuring a larger diameter and reduced width, provide space-saving benefits and efficient cooling. The choice between axial and radial flux machines depends on specific application requirements; axial flux excels in space-constrained situations like electric vehicles, while radial flux suits traditional industrial applications prioritising reliability and ease of maintenance.

### 2. Axial Flux Electrical Machines

Delving into the characteristics of stator core-less axial flux permanent machines (AFPMS). These motors offer versatile design options, including single-sided or double-sided configurations, the presence or absence of armature slots and cores, internal or external PM rotors, surface-mounted or interior PMs, and single-stage or multi-stage operation.

The chosen configuration for the prototype is a double-sided axial flux permanent magnet machine with an internal stator and no stator core. Eliminating stator cores is a distinctive feature in some AFPM designs, yielding numerous benefits. It simplifies design, enhances compactness, reduces weight, boosts power density, and minimises eddy current losses. It also improves cooling customisation, but presents manufacturing challenges and may require predictive control algorithms to keep a constant working temperature. The model under development represents an innovative three-phase axial flux motor, designed with a Y-connected winding configuration. This motor stands out with a coreless stator and twin external rotor, each equipped with powerful permanent magnets (PMs) that produce an intense magnetic field. The backing steel disc in the rotor enhances the motor's structural integrity. To comprehend this motor's performance and capabilities, several fundamental equations play a pivotal role in its analysis:

- Magnetic Flux Equation (Eq. 1):

This equation governs the magnetic induction within the motor, a fundamental factor impacting its operation.

$$\phi_f = \alpha_i B_{mg} \frac{\pi}{2p} [(D_{out}/2)^2 - (D_{in}/2)^2] \quad (1)$$

Where  $B_{mg}$  is the air gap magnetic induction produced by permanent magnets,  $p$  the number of pole pairs,  $D_{in}$  and  $D_{out}$  are the inner and outer diameters and  $\alpha_i$  is a coefficient related to the magnetic properties.

- Torque Calculation (Eq. 2):

The equation for electromagnetic torque helps assessing the ability of the motor to deliver mechanical power.

$$T_d = k_T I_a \quad (2)$$

Where  $k_T$  is the torque constant and  $I_a$  the input armature current.

- Efficiency and Power Factor Equations (Eq. 3 and 4):

$$P_{out} = P_{elm} - \Delta P_{rot} \quad (3)$$

$$\cos\phi = \frac{E_f + I_a R_1}{V_1} \quad (4)$$

Where  $P_{elm}$  is the electromagnetic power and  $\Delta P_{rot}$  represents the total rotational losses, which encompasses friction losses in bearings, windage losses, and ventilation losses (if present).  $E_f$  is the EMF,  $V_1$  the input phase voltage and  $R_1$  is the stator winding resistance.

This motor model combines innovative design with precise mathematical formulations to deliver high efficiency and performance, making it an exciting development in the field of electrical machines.

### 3. Radial Flux PMSM and Control of PM Synchronous Machines

The decision to employ radial flux motors for electric vehicle propulsion involves a careful consideration of their pros and cons. Permanent Magnet Synchronous Motors (PMSMs) emerge as a promising choice due to their high efficiency and power density. To fully leverage their potential in the development of next-generation electric vehicles, accurate analytical models and efficient optimisation techniques are essential. Delving into the mathematical model of synchronous machines reveals a cylindrical stator with a three-phase winding arrangement and a rotor equipped with permanent magnets. The electrical dynamic equations in terms of phase variables, represented by Eq. 5, 6 and 7, along with phase flux linkage components (Eq. 8, 9 and 10) involving permanent magnets, provide insights into the behaviour of the motor:

$$V_a = R_s I_a + \frac{d\Psi_a}{dt} \quad (5)$$

$$V_b = R_s I_b + \frac{d\Psi_b}{dt} \quad (6)$$

$$V_c = R_s I_c + \frac{d\Psi_c}{dt} \quad (7)$$

Where  $R_s$  is the phase resistance and  $I_a$ ,  $I_b$  and  $I_c$  are the phase currents.

$$\Psi_a = L_{aa} I_a + L_{ab} I_b + L_{ac} I_c + \Psi_{ma} \quad (8)$$

$$\Psi_b = L_{ab} I_a + L_{bb} I_b + L_{bc} I_c + \Psi_{mb} \quad (9)$$

$$\Psi_c = L_{ac} I_a + L_{bc} I_b + L_{cc} I_c + \Psi_{mc} \quad (10)$$

$L_{aa}$ ,  $L_{bb}$ ,  $L_{cc}$  are the stator self-inductances,  $L_{ab}$ ,  $L_{ac}$ ,  $L_{bc}$  the mutual inductances and  $\Psi_{ma}$ ,  $\Psi_{mb}$ ,  $\Psi_{mc}$  are the flux linkage at the stator windings due to permanent magnet.

Transitioning to the  $d$ - $q$  frame through Park's transformation unveils stator voltage equations in the  $d$ - $q$  frame:

$$v_d = R i_d + \frac{d\Psi_d}{dt} - \omega_s \Psi_q \quad (11)$$

$$v_q = R i_q + \frac{d\Psi_q}{dt} + \omega_s \Psi_d \quad (12)$$

where:

$$\Psi_q = \Psi_{aq} = L_q i_q \quad (13)$$

$$\Psi_d = \Psi_{ad} + \Psi_m = L_d i_d + \Psi_m \quad (14)$$

Where  $\Psi_m$  is the permanent magnet flux linkage. The electromagnetic torque equation (Eq. 15),  $T_e$ , demonstrates the motor's hybrid nature, combining features of conventional synchronous reluctance motors and exterior permanent magnet motors:

$$T_e = \frac{2p}{3} [\Psi_m i_q + (L_d - L_q) i_d i_q] \quad (15)$$

## 4. Thermal Sizing Methods

### 4.1. Axial Flux Motor

Based on the machine's size and the enclosures employed, various cooling configurations may be adopted for AFPM machines. In terms of cooling, AFPM machines can be categorised into two distinct groups:

- **Self-Ventilated Machines:**

In this category, cooling air is generated internally by components like rotating discs, PM channels, or similar fan-like mechanisms integrated into the machine's rotating components.

- **Externally-Ventilated Machines:**

These machines rely on external devices, such as fans or pumps, to circulate the cooling medium for temperature control. Within the externally-ventilated machines category, various cooling methods can be employed, including External Fans, Heat Pipes, and Direct Water Cooling.

Each approach offers specific advantages and considerations, contributing to the overall efficiency and performance of AFPM machines in diverse applications.

### 4.2. Radial Flux Motor

The principles governing the thermal modelling and analysis of Permanent Magnet Synchronous Motors (PMSM) are closely aligned with those applied to Axial Flux Permanent Magnet (AFPM) machines. The primary distinction lies in the thermal equivalent circuit, utilised to ascertain internal temperature distribution and model the machine's heat transfer. There exists a direct correlation between thermal and electrical parameters, fostering analogies between them. The circuit elements for representations in terms of concentrated parameters can also be interpreted as values per unit length and employed for distributed equivalents. Consequently, it is feasible to construct an equivalent thermal circuit in both cases, facilitating a comprehensive understanding of the thermal behaviour of the machines.

## 5. Motor Parameters Design

### 5.1. Axial Flux Machine Model

In developing axial flux motors, the challenge initially lays in creating an accurate model due to limited references. Using MATLAB, an equivalent model was constructed and validated with Ansys Maxwell and MotorXP software. The PNRR project partners' power and torque demands posed an intriguing challenge. After defining specifications and theoretical guidelines, the focus shifted to selecting parameters meeting these requirements. MATLAB optimisation algorithm, specifically the "fmincon" function, was employed to optimise these parame-

ters while adhering to specified constraints. The aim was to maximise efficiency, output torque, and power without resorting to trial and error procedure. Ultimately, the function returns optimised values to maximise efficiency.

The algorithm, given an initial input vector  $x_0$  and specified lower and upper bounds ( $lb$  and  $ub$ ), generates optimised values that adhere to constraints. These optimised values, compiled in Table 1, serve as inputs for a custom script to estimate output torque, power, losses, and motor parameters.

$B_r$ [T]	$\mu_{rrec}$	$t$ [mm]	$t_w$ [mm]	$h_M$ [mm]
1.125	1.051	18.00	16.00	10.53
$D_{out}$ [m]	$D_{in}$ [m]	$p$	$s_1$	$N_{ct}$
0.4000	0.2450	20	60	12
$a_w$	$d_w$ [mm]	$w_c$	$I_a$ [A]	$k_{sat}$
100	13.10	1	115.0	1
$m_r$ [kg]	$m_{sh}$ [kg]	$R_{sh}$ [mm]	$m_1$	$rpm$
15.78	0	0	3	3000

Table 1: Output optimised values that are the input for the motor model MATLAB script

Notable results include an electromagnetic torque ( $T_d$ ) of  $8.673 \times 10^2$  N m and electromagnetic power ( $P_{elm}$ ) of  $2.725 \times 10^5$  W. Key performance parameters, such as output power  $P_{out} = 2.724 \times 10^5$  W, shaft torque  $T_{sh} = 867.0$  N m, input power  $P_{in} = 2.838 \times 10^5$  W, and motor efficiency ( $\eta = 0.960$ ), satisfy the stringent requirements set by the PNRR project partners. Additional results include input phase voltage  $V_1 = 853.8$  V, line-to-line voltage  $V_{1L-L} = 1.479 \times 10^3$  V, and power factor  $\cos\phi = 0.963$ , all contributing to enhance system efficiency and performance evaluation. The design ensures sufficient stiffness for the axial flux machine, as tested virtually in Figure 1, with further validation to come in the next Chapter.

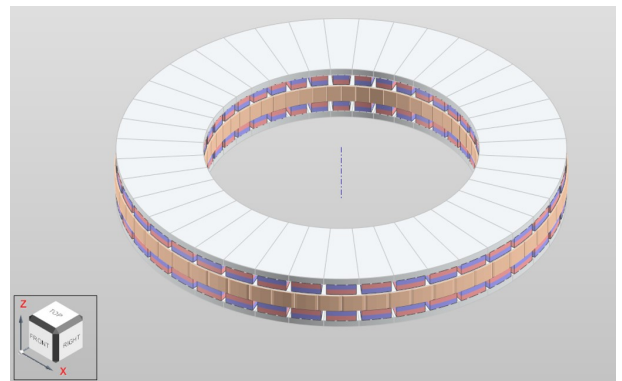


Figure 1: Virtual prototype of the developed axial flux machine model

## 5.2. Radial Flux Machine Model

The radial flux machine model, meticulously crafted and analysed through Ansys MotorCAD software, offers a comprehensive understanding when observed from its radial view, as depicted in Figure 2. This detailed perspective unveils the intricate design elements crucial to the functionality and performance of the motor. Examining the radial representation provides insights into the internal structure, arrangement of key components, and the spatial relationships among various parts, offering an in-depth understanding of the motor's construction and configuration.

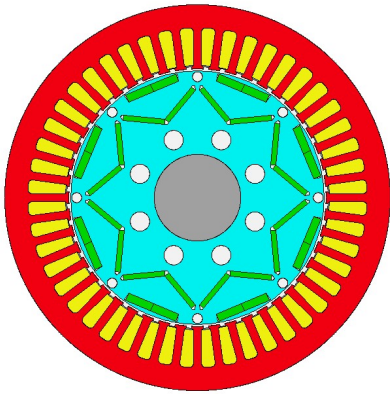


Figure 2: Radial view of the virtual prototype of the developed radial flux machine model

It not only provides a detailed look at the internal workings and dimensions, but also showcases the careful optimisation of the motor to meet stringent performance criteria. These representations collectively ensure a robust foundation for performance assessment, validation, and further refinement of the radial flux machine model. Specific features, such as the stator lamination diameter of 198 mm, a 132 mm stator bore, an air gap of 1 mm and more other aspects are intricately designed to meet the performance demands and specifications set forth for the project, ensuring optimal functionality and efficient power generation.

## 5.3. Thermal Analysis and Cooling System

The axial flux permanent magnet machine case study involves critical thermal parameters: external and internal diameters ( $D_{out} = 0.4$  m and  $D_{in} = 0.245$  m), various losses values ( $\Delta P_{rot} = 96.18$  W,  $\Delta P_e = 133.35$  W,  $\Delta P_{lw} = 1.119 \times 10^4$  W), and fluid properties. Assessing steady-state temperatures is the primary challenge, approached by segmenting the motor into distinct zones: the outer rotor disc surface, rotor disc edge, and rotor-stator system. Using the established thermal properties, an intricate thermal circuit is developed. This circuit considers

factors like radiation absence from the rotor disc to the surroundings, convection from the stator overhang to the airflow, and resistance to heat conduction between magnets and the rotor. A simplified version of this intricate circuit, showcased in Figure 3, aids in predicting the steady-state temperatures across the various components of the system.

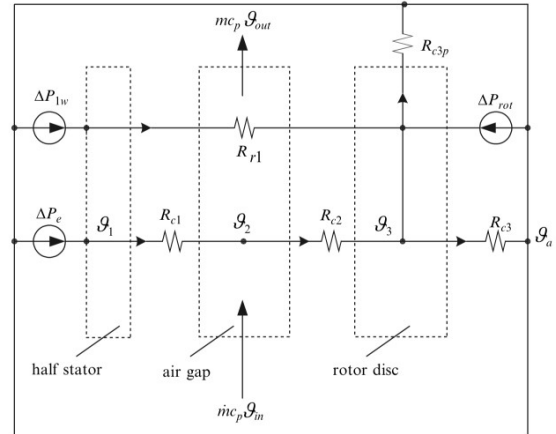


Figure 3: Simplified thermal equivalent circuit. Source: [1]

The results of the analysis of the system are:  $t_1 = 594.7^\circ\text{C}$  which represents the temperature of the stator winding,  $t_2 = 96.89^\circ\text{C}$  which is the air-gap flow temperature and  $t_3 = 97.37^\circ\text{C}$  that is the rotor disc temperature.

In the pursuit of optimal thermal control within the system, particular emphasis lies on managing the stator, recognised for operating under higher temperatures. This approach involves the utilisation of heat pipes to directly cool the motor, emphasising the convection heat transfer coefficients ( $h = 1000$  W $^\circ\text{C}/\text{m}^2$ ) on the inner surfaces of the stator heat pipes and the finned area. Critical parameters like the average convective heat transfer coefficient on the fin surfaces ( $h_{fin} = 50$  W $^\circ\text{C}/\text{m}^2$ ), finned area ( $A_{fin} = 1.8$  m $^2$ ), efficiency ( $\eta_{fin} = 0.92$ ), and the heat pipes' length within the finned surface ( $l_{fin} = 1.5$  m) are factored in. Aiming to lower the steady-state stator temperature, a heat pipe, situated along the stator's average radius, holds a designated diameter ( $D_{hp} = 0.025$  m). This design assumption considers full contact between the heat pipe's outer wall, the stator winding, and the finned surface. Assessing its effectiveness, the highest temperature among various system parts is determined through specific equations. The pre-cooling temperature, represented as  $\theta_{cold}$ , indicating the stator's steady-state temperature, is evaluated as  $219.6^\circ\text{C}$ . Exploring an alternate scenario, the impact of substituting heat pipes with a liquid cooling pipe is investigated. This liquid cooling pipe, employing a specific diameter ( $d = 0.025$  m), introduces changes



in properties like density ( $\rho$ ), specific heat constant ( $c_p$ ), dynamic viscosity ( $\mu$ ), and thermal conductivity ( $k$ ) across different types of liquids at various temperatures. The focus shifts to analysing dimensionless parameters for liquid cooling: a significant assessment that leads to the identification of optimal liquid types and concentrations. The evaluation culminates in Table 2, underscoring the stator temperatures under diverse cooling conditions, indicating the choice of 40% ethylene glycol for maintaining suitable stator temperatures within the required temperature range of average value 180 °C.

Liquid temp.	Ethylene glycol 30%	Ethylene glycol 40%	Ethylene glycol 50%
40 °C	191.1 °C	135.0 °C	73.29 °C
65 °C	247.3 °C	205.7 °C	163.6 °C
90 °C	281.9 °C	250.1 °C	219.3 °C
120 °C	288.6 °C	284.4 °C	261.7 °C

Table 2: Results of stator temperatures in different conditions

## 6. Validation of Sizing Results

### 6.1. Validation of the Axial Flux Machine Model

For a thorough validation process for the axial flux motor, two distinct and reputable software tools have been used: Ansys Maxwell and MotorXP, to cross-verify results.

Ansys Maxwell is known for its broad capabilities in complex electromagnetic analyses, offering customisation and advanced design optimisation tools, while MotorXP is specialised in electric motors, providing precise analysis specifically for axial flux motors. This combination of their strengths was crucial in accurately validating the motor, allowing for a detailed assessment of its performance and efficiency. Ansys Maxwell, an electromagnetic field solver, is suitable for a diverse range of applications from electric machines to wireless charging systems and offers specialised interfaces for electric machines and power converters. It excels in resolving static, frequency-domain, and time-varying magnetic and electric fields. It facilitates a precise understanding of nonlinear behaviour of electromechanical components and transient motion, aiding drive circuitry and control system design. The software integrates advanced field solvers with circuit and systems simulation technology, enabling in-depth comprehension of system performance before physical prototyping. The analysis involved two input currents—first, an RMS current with three sinusoidal phases, followed by a constant net zero sum current—to validate results. Examining the average output torque value, which is approximately 1200 Nm as depicted in Figure 4, it is evident that the observed value

exceeds the simulation results presented in Chapter 5.1. However, it’s important to note that this disparity can be ascribed to the initial phase misalignment between the rotor and stator, as the 3D model doesn’t achieve perfect alignment. Therefore, it is reasonable to attribute this variance in results to the inherent misalignment between these components.

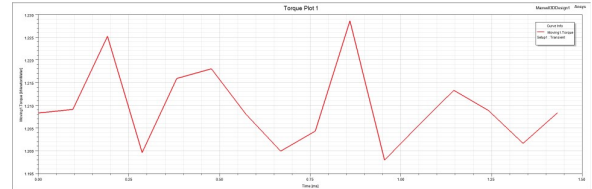


Figure 4: Output torque plot

The confirmation of results becomes even more noteworthy considering the unique features of MotorXP-AFM. It stands as the singular software exclusively tailored for the electromagnetic design and assessment of axial flux machines (AFM) with permanent magnets, covering brushless DC and permanent magnet synchronous motors and generators. Its innovative quasi-3D finite element modelling approach redefines AFM design, achieving computational speeds nearly ten times faster than full 3-D FEA, without compromising precision. Offering a diverse range of analysis types and over a hundred output parameters, along with customisable templates, a rich material library, and an optimisation API, MotorXP-AFM establishes a flexible and robust e-machine design workflow. Accessible as both a MATLAB-based application and a standalone program, it stands as a versatile and independent tool for engineering analysis.

### 6.2. Validation of the Radial Flux Machine Model

The validation of the radial flux machine model was executed using Ansys’ Motor-CAD, which is a software that enables engineers to evaluate diverse motor designs across their operational spectrum. Motor-CAD’s four modules (EMag, Therm, Lab, and Mech) enable rapid multiphysics calculations, expediting the design process from concept to the final product. This approach significantly reduces the time needed for design iterations, allowing to model a motor enhancing performance, efficiency, and compactness. The most noteworthy plot in this chapter is the torque (Figure 5), as it remains the focal point of this analysis throughout. Comparing axial and radial flux motor models, it’s clear that the radial design is larger and tends to offer lower performance for the same power output. Specifically, its torque is nearly half that of the axial design, emphasising the compactness and torque efficiency advantages of the axial flux motor.

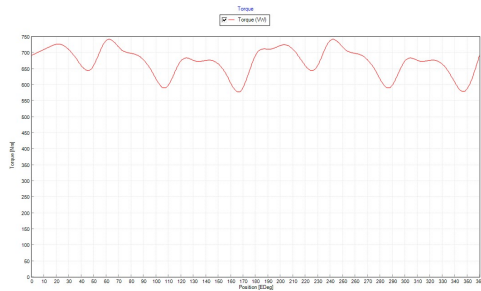


Figure 5: Torque plot, average value: 700Nm

### 6.3. Validation of the Cooling System Design

#### 6.3.1 Axial Flux Motor Case

ANSYS Fluent, a powerful Computational Fluid Dynamics (CFD) software, is widely utilized for simulating fluid flow and heat transfer phenomena in engineering applications. In this thesis, Fluent is employed to validate thermal analysis results for axial-flux motors with liquid cooling. The software's sophisticated capabilities ensure accuracy in assessing the thermal performance of such systems. The simulation focuses on heat distribution in temperature-sensitive motor components, particularly the winding sections, and considers heat exchange between tubes and the stator. A deliberate cut in the tubes replicates fluid entry, crucial for real-world fluid dynamics. The simulation uses a 40% ethylene-glycol solution at 50 °C. The results, illustrated in Figure 6, show convergence and a peak temperature of 413 K, aligning with estimated values in Table 2 and below the PNRR project partner's specified limit of 180 °C.

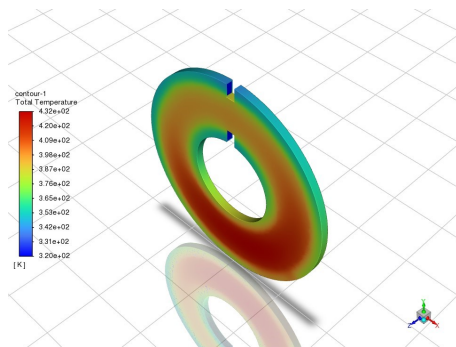


Figure 6: Contour figure of the thermal distribution in stator and cooling pipes

#### 6.3.2 Radial Flux Motor Case

MotorCAD simplifies thermal analysis by incorporating housing and fins, using finite element analysis to map temperature distribution within the motor. It automates the creation of an equivalent thermal circuit and schematic, offering a detailed view of thermal distribution in the windings (Figure 7):

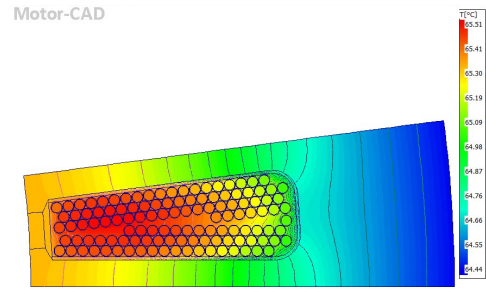


Figure 7: Thermal finite element analysis, windings view

These analyses reveal that internal motor temperatures stabilise around 65 °C even without liquid cooling, a notable advantage for radial flux motors. Radial flux motors also benefit from more temperature control studies, aiding in designing efficient cooling systems for maintaining optimal operating temperatures.

## 7. Conclusions and Future Developments

The PNRR project source of this thesis is a 3-year initiative aimed at producing various prototypes of electric motors for automotive applications. The primary objective is to facilitate the transition to electric propulsion and enhance its efficiency, especially in a context where Italy remains somewhat sceptical about electric vehicles.

The thesis addresses crucial initial steps in designing these motors, emphasising iterative optimisation, steady-state thermal analysis, and validation of the axial and radial flux motor models. In this process, several new programs have been employed, including tools like MATLAB for model generation, ANSYS Maxwell and MotorXp for result validation, and ANSYS Fluent for thermal result validation. The question of which motor type is superior, axial or radial flux, remains complex to answer definitively. The choice largely depends on the specific application, the axial flux design shows promise in the automotive sector. However, challenges, such as limited research on adaptive cooling, persist.

Future steps to be followed to complete this project, involve a more comprehensive transient temperature analysis, exploring predictive control methods like Model Predictive Control, integrating systems, producing a physical prototype, and ensuring compliance with industry standards for long-term reliability and performance.

## References

- [1] J. F. Gieras, R.-J. Wang, and M. J. Kamper. *Axial Flux Permanent Magnet Brushless Machines*. Springer Dordrecht, 2<sup>nd</sup> edition, 2008.